Deep time diversity and the early radiations of birds

Yilun Yu[a,b], Chi Zhang[a,c,1], and Xing Xu[a,c,1]

[a]Key Laboratory of Vertebrate Evolution and Human Origins, Institute of Vertebrate Paleontology and Paleoanthropology, Chinese Academy of Sciences, Beijing 100044, China; [b]Yuan Pei College, Peking University, Beijing 100871, China; and [c]Center for Excellence in Life and Paleoenvironment, Chinese Academy of Sciences, Beijing 100044, China

Edited by Neil H. Shubin, University of Chicago, Chicago, IL, and approved January 5, 2021 (received for review October 11, 2020)

Reconstructing the history of biodiversity has been hindered by often-separate analyses of stem and crown groups of the clades in question that are not easily understood within the same unified evolutionary framework. Here, we investigate the evolutionary history of birds by analyzing three supertrees that combine published phylogenies of both stem and crown birds. Our analyses reveal three distinct large-scale increases in the diversification rate across bird evolutionary history. The first increase, which began between 160 and 170 Ma and reached its peak between 130 and 135 Ma, corresponds to an accelerated morphological evolutionary rate associated with the locomotory systems among early stem birds. This radiation resulted in morphospace occupation that is larger and different from their close dinosaurian relatives, demonstrating the occurrence of a radiation among early stem birds. The second increase, which started ∼90 Ma and reached its peak between 65 and 55 Ma, is associated with rapid evolution of the cranial skeleton among early crown birds, driven differently from the first radiation. The third increase, which occurred after ∼40 to 45 Ma, has yet to be supported by quantitative morphological data but gains some support from the fossil record. Our analyses indicate that the bird biodiversity evolution was influenced mainly by long-term climatic changes and also by major paleobiological events such as the Cretaceous–Paleogene (K–Pg) extinction.

birds | biodiversity | radiation | diversification rate | morphological evolution

The evolution of global biodiversity is a focal area of study in both evolutionary biology and paleontology, but its examination has been approached in different ways. Neontological studies reconstruct the history of biodiversity mainly by analyzing the tempo and mode of diversification based on molecular timetrees composed of extant species (1). By contrast, paleontologists normally measure past biodiversity by investigating morphological evolution and taxic diversity from the fossil record (2). This dichotomy in both methodology and data sources is best exemplified by recent studies on the evolution of bird biodiversity (the vernacular term "birds" is equivalent to the phylogenetic taxon "Avialae" in the present paper; see *Methods* and *SI Appendix*, Supplemental Text A). For example, the time-calibrated phylogeny of extant birds and related diversification rate analyses have revealed a rapid diversification of crown birds (equivalent to the phylogenetic taxon "Aves") near the Cretaceous–Paleogene (K–Pg) boundary followed by a period of low-level net diversification rates starting about 50 Ma (3–5). Paleontological studies have revealed high morphological evolutionary rates both prior to and after the origin of Avialae (6–14), and an increased taxonomic diversity in the Early Cretaceous based on the known Mesozoic fossil record (15) (*SI Appendix*, Supplemental Text B). However, these results are not directly comparable and are difficult to be evaluated within the same evolutionary framework given that they are based on different evaluation parameters of bird diversity.

Results and Discussion

Bird Lineage Diversification Rate through Time. Lineage diversification rate through time (DRTT) analyses are widely applied to examine the history of biodiversity using molecular data but are rarely implemented in paleontology in part because few analytical tools are available. The only two studies relevant to DRTT of stem birds have produced contradictory results (6, 16). One study suggests an accelerated diversification rate for early stem birds (6), but the other study reveals no such increase (16). Here, we assembled three informal supertrees that combine the published phylogenies (3, 5, 9, 11–14) of both stem- and crown-group birds (here referred to as Supertrees 1 through 3, which contain 331, 300, and 300 taxa, respectively; see *Methods* and *SI Appendix*, Figs. S1–S5 and Supplemental Text C; stem birds refer to nonavian avialans) in order to infer the diversification rate shifts over time by utilizing Bayesian phylogenetic approaches under the skyline fossilized birth–death (SFBD) model. This approach has the advantage of modeling the evolutionary process explicitly and incorporating diverse data sources while taking into account uncertainties in the parameters, a feature absent among the methods applied in previous studies on the biodiversity of other extinct groups including stem birds (6, 16). Importantly, the SFBD model considers both extinction events and fossil sampling, two important factors for reconstructing diversification dynamics which previous studies ignored (see *Methods* and *SI Appendix*, Supplemental Text D).

It should be noted that there are debates about whether a correlation exists in evolutionary rates across different types of data and between morphological and molecular evolution and lineage diversification (17–23). For example, among vertebrates, a correlation has been found between morphological evolution and speciation rate in ray-finned fishes (24) and species richness or speciation rate in birds (25, 26), between morphological evolution and species richness in salamanders (27), and between molecular evolution and species richness and diversification rate in birds and reptiles (28, 29). However, a correlation has not been detected between morphological and molecular evolutions in mammals (30), between morphological evolution and diversification rate in

Significance

Our lineage diversification rate through time analyses of three supertrees combining the published phylogenies of both stem and crown group birds reveal three distinct large-scale increases in the diversification rate across bird evolutionary history. The first two increases also are associated with rapid morphological evolution pertaining to the locomotory and cranial systems, respectively. The third increase needs further support from morphological data. Our study demonstrates that the bird biodiversity evolution was influenced mainly by long-term climatic changes and also by the Cretaceous–Paleogene extinction.

Author contributions: Y.Y., C.Z., and X.X. designed research; Y.Y, C.Z., and X.X. performed research; C.Z. contributed new reagents/analytic tools; Y.Y. analyzed data; and Y.Y., C.Z., and X.X. wrote the paper.

The authors declare no competing interest.

This article is a PNAS Direct Submission.

[1]To whom correspondence may be addressed. Email: zhangchi@ivpp.ac.cn or xu.xing@ivpp.ac.cn.

This article contains supporting information online at https://www.pnas.org/lookup/suppl/doi:10.1073/pnas.2019865118/-/DCSupplemental.

Published February 22, 2021.

salamanders (23), squamates (22), and mammals (31), and between molecular evolution and diversification rate in mammals (32). This complexity cautions estimating diversification rate based on combined datasets of different types. However, there is empirical evidence supporting the correlation between morphological and molecular evolution and diversification rate in reptiles and birds (25, 26, 28, 29). Furthermore, we also have considered this factor by applying different (and independent) evolutionary models for morphological and molecular evolution when building Supertrees 1 through 3, and the lineage diversification rates were calculated based on the supertrees and corresponding node and tip ages in the trees, independent of the morphological and molecular data (*SI Appendix*, Supplemental Text E).

Our DRTT analyses reveal the same diversification patterns in Supertrees 1 through 3, and this pattern remains unchanged under various prior assumptions (see *Methods* and *SI Appendix*, Supplemental Text D). Specifically, we recover three distinct large-scale net diversification rate increases across bird evolutionary history (Fig. 1 *A*–*C* and *SI Appendix*, Figs. S6–S8). The first increase began between 160 and 170 Ma and reached its peak between 130 and 135 Ma. The second increase started ∼90 Ma and reached its peak between 65 and 55 Ma, though the majority of this increase is complex (e.g., the increase is fluctuating between 90 and 70 Ma and there is a harsh drop during 65 to 70 Ma). The third large-scale increase occurred after ∼40 to 45 Ma. Our results are similar to the collective results from previous studies of the lineage diversification rate for stem and extant birds (3, 4, 6) in revealing these three distinct large-scale lineage diversification rate increases, but they also display some differences to previous studies. For example, the only study revealing an accelerated diversification rate for stem birds was unable to show when the rate shifts occurred and what the rates are because of limitations in the methodology (6). The DRTT analyses of crown birds alone do not reveal a distinct decrease in lineage diversification rate around the K–Pg extinction (3, 4), an event considered to have a large impact on the biodiversity of birds as well as many other organismal groups (13, 33). However, it should be noted that our study also was unable to detect a decrease in lineage diversification rate between ∼25 and 10 Ma revealed by some previous studies (3), and that may result from the assumption of random sampling of extant species used in our analyses.

To investigate the previous failures to reveal a decrease in lineage diversification rate around 66 Ma (3, 4), we ran the analyses on Supertrees 1 through 3 with all fossil species of crown birds excluded. The results still display a distinct decrease of net diversification rate between 70 and 65 Ma (Fig. 1 *D*–*F*), suggesting that the known fossil record of crown birds has no major effect on reconstruction of the lineage diversification rate around the K–Pg boundary. We further excluded *Vegavis* and the Late Cretaceous stem birds from ref. 13 and reran the analyses using only the backbone trees of Supertrees 1 through 3. Interestingly, the results show a continuous increase in the net diversification rate across the K–Pg boundary rather than a large drop (Fig. 1 *G*–*I*). These analyses thus demonstrate that stem bird fossils rather than crown bird fossils have the critical impact on the diversification rate estimation around K–Pg boundary, and the failure to reveal a decrease in the lineage diversification rate during the K–Pg extinction event is likely the result of the limited fossil sampling of Late Cretaceous stem birds, not of crown birds. In other words, it is stem birds that contribute to the main bird diversity around the K–Pg boundary, consistent with the known paleontological data (13, 34–36) and most recent time-calibrated phylogenetic hypotheses of extant birds (3–5, 37, 38). Nevertheless, our analyses demonstrate that fossil data have different effects on the study of speciation, extinction, and sampling rates in different time intervals (*SI Appendix*, Figs. S9–S11), during which stem and crown birds contribute differently to the overall biodiversity.

We also ran the analyses on Supertrees 1 through 3 using the lineage-specific multitype birth–death (MTBD) model (39) implemented in Beast2 (40). Unlike the SFBD model, the MTBD model assumes that different lineages or clades can have different speciation and extinction rates (39, 41). The analyses revealed multiple diversification rate shifts among crown birds but failed to detect any diversification rate shift among stem birds (*SI Appendix*, Figs. S12–S20). This might have been caused by the inconsistency between model assumptions. Most notably, the MTBD model favors only large rate changes and the sampling rate of extinct species is constant over time (39, 41), while the actual fossil record of birds suggests variable rates in bird evolution (42). In this case, the shift in net diversification rate could be inferred inaccurately (41). Consequently, we chose to accept the results from the analyses based on the SFBD model for our discussion on bird biodiversity evolution (see *Methods* and *SI Appendix*, Supplemental Text D).

Morphological Evolution of Birds. The increases in the lineage diversification rate suggest three radiations are present in bird evolution, and we further tested this hypothesis by examining the morphological evolutionary rate along the lineage to extant birds. We did not perform the morphological evolutionary rate analyses on Supertrees 1 through 3 because the relevant morphological data for most of the taxa in Supertrees 1 through 3 are not available and also because it is important to compare the morphological evolutionary rates of stem birds with those of their close dinosaurian relatives (which are absent in Supertrees 1 through 3) in order to better understand the radiation among early stem birds. Consequently, we used a comprehensive character matrix from ref. 7, with a slight modification (we deleted five wildcard taxa and added a newly discovered taxon), which includes 853 characters coded across 148 species of both stem and crown birds and other coelurosaurian theropods (see *Methods* and *SI Appendix*, Supplemental Text F).

Our analyses of the morphological data matrix based on different relaxed clock models produced a similar pattern for the morphological evolution of birds and their close dinosaurian relatives. Morphological evolution is rapid along the internal branches between the Tyrannoraptora and Ornithothoraces nodes and is slow along the internal branches crownward of the Ornithothoraces node (Fig. 2*A* and *SI Appendix*, Figs. S21*A* and S22*A*). The high morphological evolutionary rates along the phylogenetically earliest internal branches of birds (PEIBB) provide further support for the occurrence of a radiation among early stem birds.

However, the morphological evolutionary rate is slightly lower along PEIBB than along the internal branches between the Tyrannoraptora and *Archaeopteryx* + Pygostylia nodes (Fig. 2*A* and *SI Appendix*, Figs. S21*A* and S22*A*). To further understand the morphological evolution pertaining to the origin of birds, we ran the analyses on the partitioned data matrix (i.e., the skull, axial skeleton, pectoral girdle, forelimb, pelvis, and hindlimb). Our analyses indicate that morphological evolutionary rates in different anatomical regions were extremely heterogenous during coelurosaurian evolution (Fig. 2 *B*–*G*). Compared to most other coelurosaurian lineages (including most bird lineages), the PEIBB have considerably higher evolutionary rates in the pectoral girdle, forelimb, and hindlimb (Fig. 2 *D*, *E*, and *G* and *SI Appendix*, Figs. S21 *D*, *E*, and *G* and S22 *D*, *E*, and *G*), and the branch between the Aves and Neognathae nodes also displays a relatively high evolutionary rate in the skull (Fig. 2*B* and *SI Appendix*, Figs. S21*B* and S22*B*). We further examined coelurosaurian morphological evolution under different phylogenetic constraints and relaxed clock models. The recovered patterns of evolution in the postcranial skeleton are strong, and those in the cranial skeleton vary slightly under different assumptions (see *Methods* and *SI Appendix*, Supplemental Text F).

In a broader view, our analyses revealed two peak rates of coelurosaurian morphological evolution along the branches leading

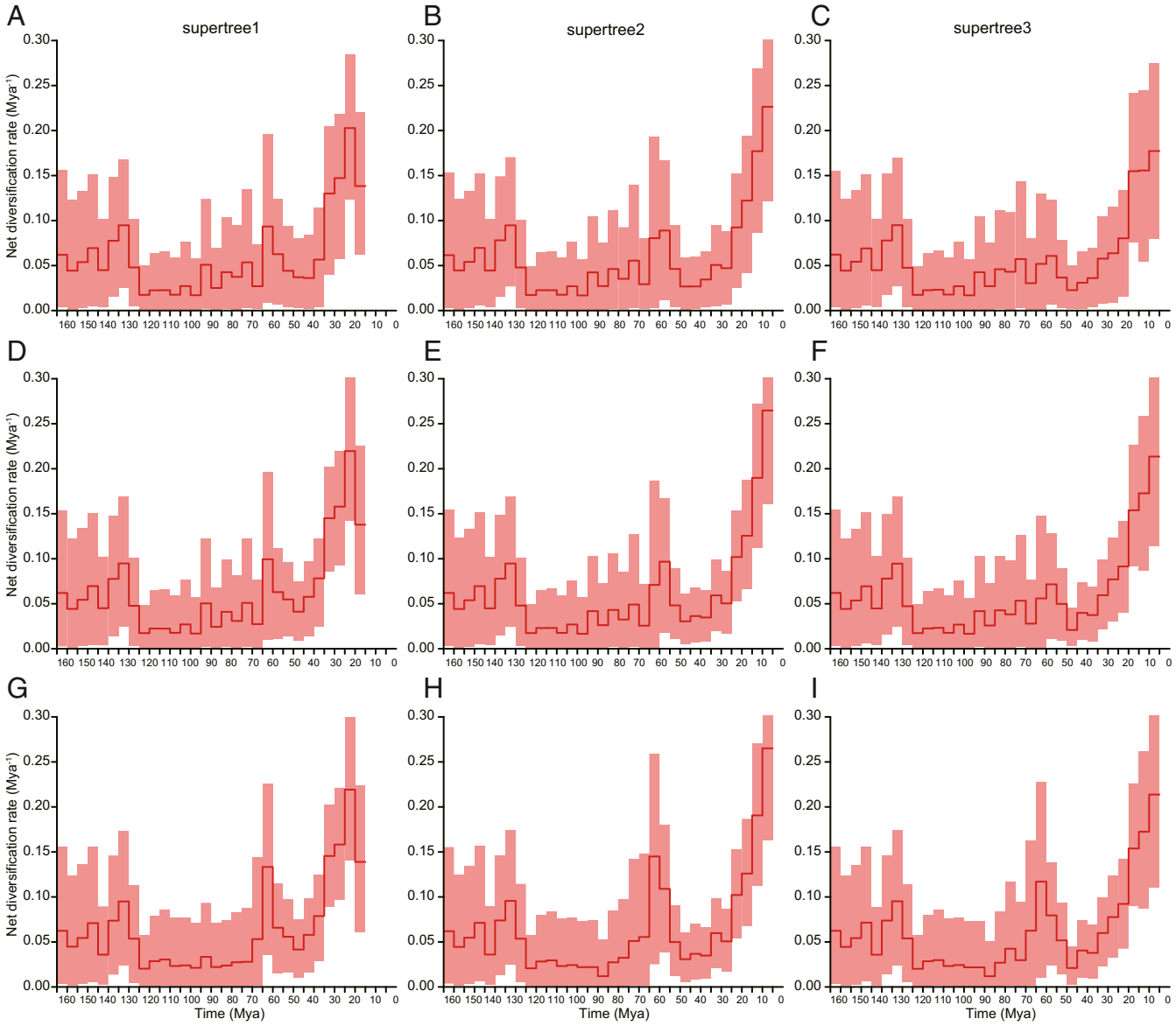

Fig. 1. Diversification of birds through time. Estimates of the tree-wide lineage net diversification rate calculated in 5-My intervals (line segments) based on Supertree 1 (*A*), Supertree 2 (*B*), and Supertree 3 (*C*). (*D–F*) are based on supertrees without fossil crown birds and (*G–I*) on the three backbone supertrees. The rates at the last three time intervals for Supertree 1 and at the last interval for Supertrees 2 and 3 are not shown in the figures because of the absence of branching events resulting in model violation and inaccurate rate estimates. The rates were estimated under default prior assumptions (*SI Appendix*, Supplemental Texts C–E). The red boxes around medians are 95% highest posterior density (HPD) intervals.

to the origins of Maniraptoriformes and Pennaraptora, respectively (Fig. 2*A*), representing two important evolutionary events along the line to birds. These two peaks differ in which skeletal regions were involved and how fast these skeletal regions evolved. The first peak is linked with accelerated evolution in the cranial and axial skeleton (Fig. 2 *B* and *C* and *SI Appendix*, Figs. S21 *B* and *C* and S22 *B* and *C*) and the second peak with comparatively rapid evolution in the postcranial skeleton (Fig. 2 *C–G* and *SI Appendix*, Figs. S21 *C–G* and S22 *C–G*). These two peaks also are associated with significant changes pertaining to diet, locomotion, and physiology in coelurosaurian evolution (43–45) (Fig. 2 and *SI Appendix*, Supplemental Text G and Figs. S21 and S22). These peaks are consistent with previous qualitative analyses, which suggest the origin of some major bird characteristics well before the origin of Avialae (43).

Finally, we compared the morphological disparity and morphospace occupation of birds and other coelurosaurian clades based on the same character matrix (Fig. 3). When the unpartitioned data matrix is used to calculate a distance matrix and compare morphological disparity, most tests are significant regardless of whether or not crown birds are included and which distance matrix is used (*SI Appendix*, Supplemental Text H). This result demonstrates that stem birds occupy a larger morphospace than other coelurosaurian clades (Fig. 3*A*). When the matrix is partitioned, stem birds are not significantly different from other coelurosaurian clades in cranial, axial, and pelvic morphospaces (Fig. 3 *B*, *C*, and *F* and *SI Appendix*, Figs. S23–S25 *B*, *C*, and *F*, S27, S28, S31, S34, S35, and S38 and Tables S1 and S2), but they have a significantly larger morphospace in the pectoral girdle, forelimb, and hindlimb datasets (Fig. 3 *D*, *E*, and *G* and *SI Appendix*, Figs. S23–S25 *D*, *E*, and *G*, S29, S30, S32, S36, S37, and S39 and Tables S1 and S2). Most results of the permutational multivariate analysis of variance (PERMANOVA) are significant,

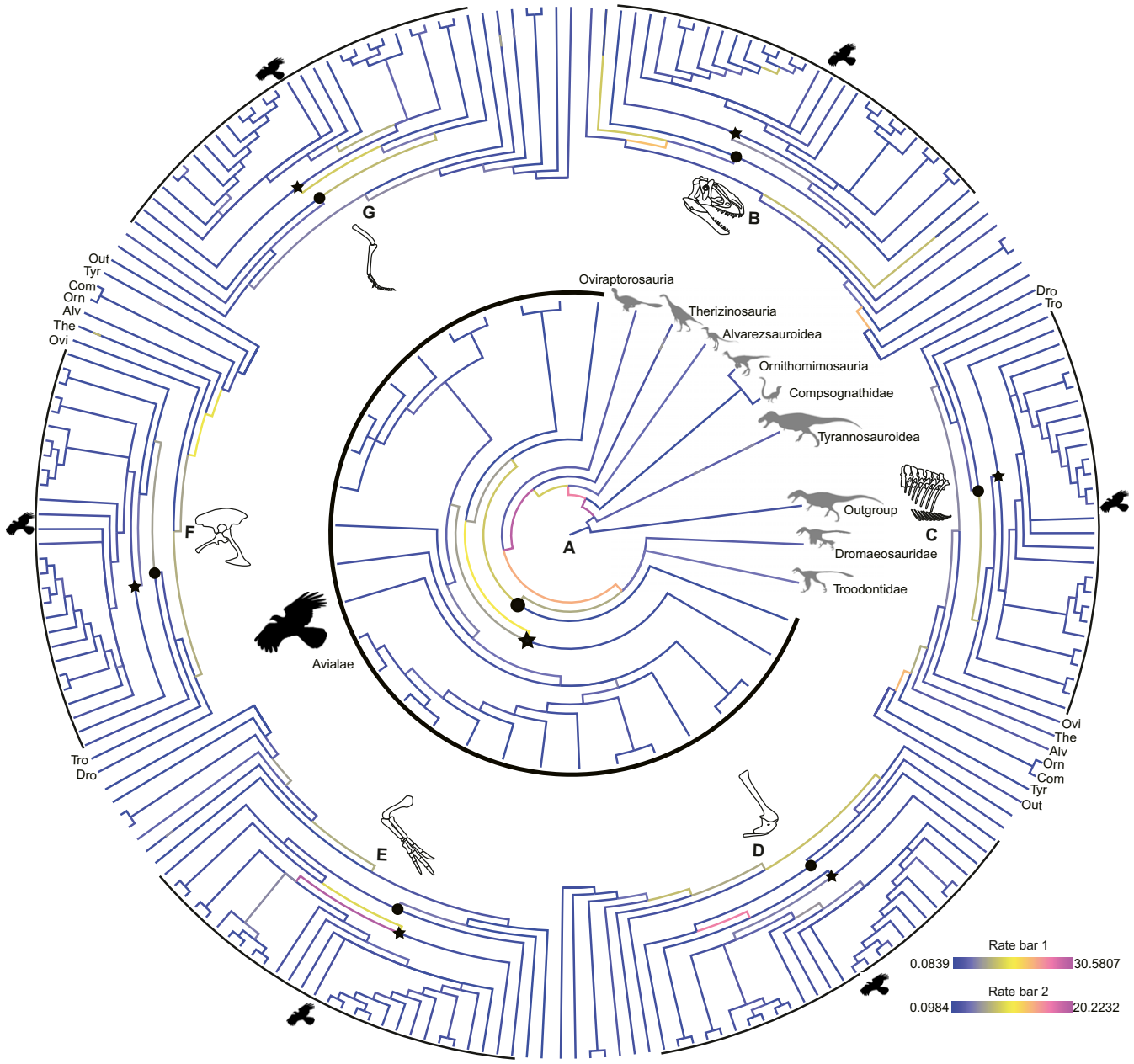

Fig. 2. Simplified cladograms showing morphological evolutionary rates of birds and nonavialan dinosaurs based on the WN relaxed-clock model without any extra phylogenetic constraint. This figure is derived from *SI Appendix*, Fig. S21 by collapsing all nonavialan dinosaurian clades into single branches with the relative position of rate shifts in these clades denoted with short colored bars. The black circles represent Avialae and the black stars represent Pygostylia. The rates presented in the cladograms were estimated from an unpartitioned character matrix (*A*) and a partitioned character matrix of skull (*B*), axial skeleton (*C*), pectoral girdle (*D*), forelimb (*E*), pelvis (*F*), and hindlimb (*G*) (*SI Appendix*, Supplemental Texts F and G). Rate bar 1 for (*A*) and rate bar 2 for (*B*–*G*). Abbreviations: Out, Outgroup; Tyr, Tyrannosauroidea; Com, Compsognathidae; Orn, Ornithomimosauria; Alv, Alvarezsauroidea; The, Therizinosauria; Ovi, Oviraptorosauria; Tro, Troodontidae; Dro, Dromaeosauridae. Silhouettes are from http://phylopic.org/.

and nearly all results of the comparative distance test are significant, indicating that birds occupy a different area in the multivariate morphospace as compared to that of other coelurosaurians in all six anatomical regions (Fig. 3 and *SI Appendix*, Figs. S23–S25 and Tables S3 and S4). In other words, birds are a notable outlier in coelurosaurian morphospace. This conclusion remains robust with crown birds excluded, the phylogenetic uncertainty of several taxa, and using different distance matrices (*SI Appendix*, Supplemental Text H).

Previous studies also show the general, rapid morphological evolutionary rates among early stem birds (6–10, 46–48). However, they differ from our study in providing no information on which anatomical regions evolved comparatively faster among early stem birds because of the lack of partitioned analyses (7–9). They reveal no difference in evolutionary rates among the different anatomical regions (46), or indicate high evolutionary rates among early stem birds in those anatomical regions [e.g., axial skeleton (10), hindlimb (6, 47), or pelvic girdle (49)] different from our study (the whole locomotory system, particularly the flight apparatus). Two studies comparing the morphological disparity between Mesozoic birds and other theropod dinosaurs (6, 7), including the one upon which the dataset for our analyses is based (7), failed to reveal a larger and

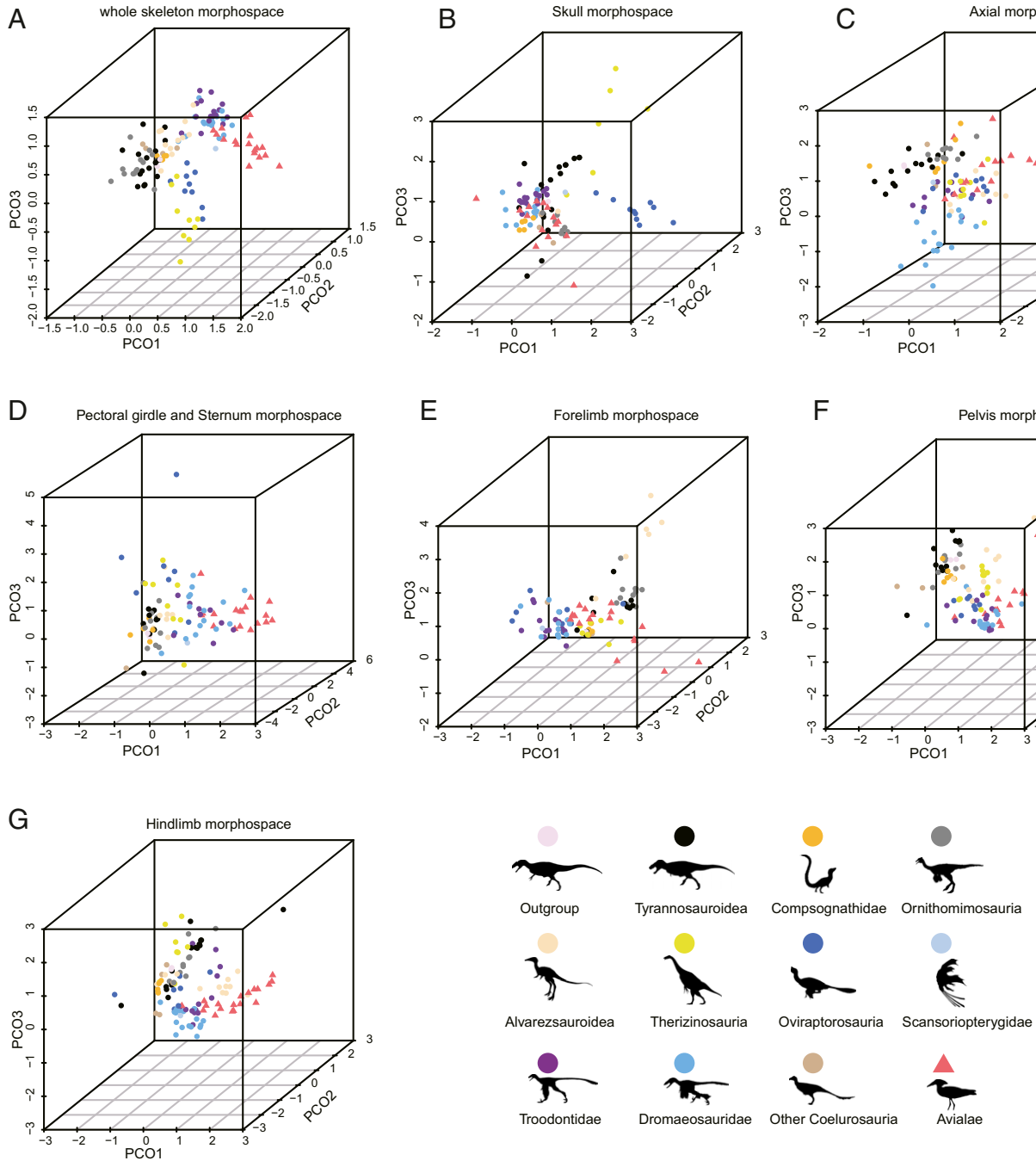

Fig. 3. Morphospace comparisons of stem birds and other coelurosaurian clades based on the results of the disparity analyses of MORD matrices. Nonavialan dinosaurs are denoted with colored circles and birds are denoted with red triangles. The comparisons are based on whole skeleton (*A*), skull (*B*), axial skeleton (*C*), pectoral girdle (*D*), forelimb (*E*), pelvis (*F*), and hindlimb (*G*) morphospaces (*SI Appendix*, Supplemental Text H). Silhouettes are from http://phylopic.org/.

different morphospace for stem birds as compared to nonavialan theropods (*SI Appendix*, Supplemental Text B and H). It should be noted that one published abstract revealed a larger disparity among stem birds in the anatomical modules [all postcranial regions (49)] different from our study (forelimb, pectoral girdle, and hindlimb).

Biodiversity Evolution and Climate-Induced Vicariance and the K–Pg Extinction Impact. Our analyses of lineage divergence rates for birds suggests the presence of at least three major radiations in bird evolution (Fig. 1), and our analyses of morphological evolutionary rate for birds provide further support for the first two radiations (i.e., the one among early stem birds and the one among early neognathous birds; Fig. 2). The presence of the first radiation is supported further by our morphological disparity analyses (Fig. 3 and *SI Appendix*, Fig. S40). Our morphological evolutionary rate and disparity analyses both indicate that the key structures for flight, including the forelimb and pectoral girdle of early stem birds, evolved at much higher rates as compared to those of their close dinosaurian relatives (Figs. 2 *D* and *E* and 3 *D* and *E*), suggesting that the first radiation probably relates to the invasion of a new ecospace (i.e., aerial space). Previous morphometric studies also suggest that the functional

disparity of the forelimb and pectoral girdle skeleton in Mesozoic birds is large (50–53). These presumably aerial adaptations were probably influenced by the selective extinction of small-sized nonpterodactyloid pterosaurs near the Jurassic–Cretaceous boundary (54).

The second radiation is associated with cranial modifications, which probably are related to a diversification in diet and foraging behavior (11, 55), and that difference likely suggests that the selection on the skeleton during the second radiation was different from that of the first radiation (Fig. 2 and *SI Appendix*, Fig. S40). However, from the perspective of morphological evolution, comparatively limited morphological data and taxon sampling for crown birds in our analyses might not be able to fully illuminate the evolutionary signals for early crown birds. For example, besides cranial modifications, pedal specializations for different ecological roles also appeared quickly among early crown birds (12), but that change was not detected by our analyses. Future morphology-based analyses for early crown birds are thus required to better understand the second radiation.

The third radiation occurring after ∼40 to 45 Ma is indicated by our DRTT analyses, as well as previous DRTT studies (3, 4), but our morphological evolution analyses are unable to provide support for this radiation given the limited morphological dataset used in our analyses. Nevertheless, this third radiation (near in time to the Eocene–Oligocene boundary and its associated global cooling event) previously has been proposed based on molecular data (56, 57) and seems to have some support from the fossil record (58). However, improved fossil sampling and sample sizes around Eocene–Oligocene transitional period is required to better understand and document this hypothesized radiation.

While from the perspectives of functional morphology and ecology, the radiations of early stem and early crown birds appear to have derived from different factors in selection, and our reconstructed lineage diversification rates of birds are in general negatively correlated with recently published global temperature curves from the Jurassic to the recent (59, 60) (*SI Appendix*, Fig. S41). Previous studies have suggested that the diversity of crown birds was driven by climate-induced vicariance (3). In other words, the net diversification rate increased during cooling periods as the result of the fragmentation of megathermal forests and decreased during warm periods attributed to the expansion of megathermal forests and connectivity with homogenization of avifaunas (3). Our analyses provide further support for this interpretation and indicate that the diversity of stem birds was probably similarly derived. Global temperatures dropped from the Late Jurassic into the Early Cretaceous (59, 60). That temperature change likely resulted in fewer megaplants and patchier forests, and that idea is supported by paleobotanical evidence (61, 62). This botanical change might have facilitated allopatric speciation of stem birds and led to the first major radiation in bird evolution. Multiple lines of evidence including molecular systematics and fossils suggest the expansion of megathermal forests during the middle Cretaceous (63–66). This forestation might have contributed to the low net diversification rates in birds during the middle Cretaceous. Slowdowns in lineage diversification during this period also are known in some other terrestrial animals such as most Mesozoic ground-living dinosaurs (16), and they suggest that the middle Cretaceous super greenhouse climate had a major impact on the terrestrial vertebrate evolution. However, the evolution of some terrestrial vertebrate groups including mammals and some dinosaurian groups such as ceratopsians and hadrosauroids displays a different pattern. Their biodiversity, functional morphology, and ecology are suggestive of a radiation possibly linked with the increased plant diversity during the middle Cretaceous super greenhouse climate (16, 67, 68). This pattern suggests that different animal groups have been affected differently by past climate changes and plant evolution.

There is strong evidence for the diversification of stem birds immediately before the K–Pg boundary (13, 34–36), as well as the subsequent radiation of crown birds in the earliest Paleogene (12, 34–36), as revealed by our DRTT and morphological evolution rate analyses (Figs. 1 and 2). The Late Cretaceous increase in lineage diversification rate revealed by our analyses is likely related to the fragmentation of megathermal forests during the Late Cretaceous cooling event (69), and a long-term cooling event is absent in early Paleogene. Thus, the early radiation of crown birds was probably not influenced by long-term climatic-induced vicariance. More likely, it is the K–Pg extinction with its related ecological and environmental changes that is responsible for the evolution of bird diversity around the K–Pg boundary. The extinction wiped out stem birds and the volant pterosaurs, providing an ecological release (13, 70), and this change facilitated the radiation of crown birds in the earliest Paleogene (3, 13).

Conclusions

Our DRTT analyses under the SFBD model on a combined dataset of crown and stem birds, together with the morphological evolution analyses, reveals a number of interesting evolutionary patterns of bird diversification dynamics, some of which are not revealed or well documented in previous studies. Previous studies demonstrate that there are identifiability issues with the model's parameters when only extant (71) or extinct (72) species are used in the analyses. However, our analyses that combine both the extinct and extant species (such as the SFBD model in Bayesian framework) are not influenced by the identifiability issues. Our study provides further support for the central role of fossil data in understanding macroevolutionary patterns and processes, including diversification dynamics, and in particular for the questions related to the evolution of stem groups or deep divergences of crown clades. Our results demonstrate the importance of the integration of both data and methodology in understanding the macroevolution of major organismal groups, and particularly those groups with a long history of extinct stem taxa already possessing the characteristic, innovative apomorphic morphologies and ecologies of its living relatives. However, our study also highlights some issues for future studies using the integrated approach to understanding macroevolution. For example, we demonstrate how to combine different types of data and how to choose different measures, models, and statistical methods that are important and seem to be clade-specific and variable for different questions. This approach requires not only expertise across multiple disciplines but also further development of relevant methodologies (*SI Appendix*, Supplemental Text D and E).

Methods

Time-Scaled Informal Supertree Assembly. We assembled Supertrees 1 through 3 by combining published bird phylogenies (3, 5, 9, 11–14). First, we assembled three backbone trees (*SI Appendix*, Fig. S4 *C* and *D*) by combining respectively the stem bird phylogeny in ref. 9 to three crown bird phylogenies (i.e., the molecular-clock calibrated tree in ref. 3 and two molecular-clock calibrated trees in ref. 5). The median root age of the tree in ref. 3 is 92.5 Ma. Tree one in ref. 5 is given in the main text of ref. 5, and its median root age is 72.9 Ma. Tree two in ref. 5 is given in the SI Appendix of ref. 5, and its median root age is 78.4 Ma. Both trees are Bayesian trees. The first tree did not use *Vegavis* as a fossil calibration point. The second tree included *Vegavis* as a fossil calibration point, and hence the estimates of node ages and branch lengths are different between the two trees. The molecular-clock calibrated tree in ref. 3 and the stem bird tree in ref. 9 are combined to assemble Supertree 1; molecular-clock calibrated tree one and tree two in ref. 5 and the stem bird tree in ref. 9 are respectively combined to assemble Supertree 2 and Supertree 3. The divergence times of the stem birds were estimated using a Bayesian tip-dating approach on the fixed topology. The fossil ages were assigned uniform priors with lower and upper bounds from the corresponding stratigraphic ranges. Second, we added the following 48 additional fossil birds to each of the three backbone trees: 18 Late Cretaceous stem birds from the Adams consensus tree in ref. 13 (*SI Appendix*, Fig. S4*E*), 1 stem bird and 11 crown birds from the

maximum parsimony tree in ref. 11 (*SI Appendix*, Fig. S4*F*), 11 crown birds from the Bayesian maximum clade credibility tree in ref. 14 (*SI Appendix*, Fig. S4*A*), and 7 crown birds from the tree with backbone constraints in ref. 12 (*SI Appendix*, Fig. S4*B*).We estimated the divergence times of these fossil birds using the same tip-dating approach on the fixed topologies from these references. The fossil ages in the subsequent tip-dating analyses were given fixed values as the posterior medians if they had been estimated already in previous runs. The other fossil ages were assigned uniform distributions with lower and upper bounds collected from the Paleobiology Database (PBDB). Node calibrations were enforced if they were necessary to reconcile with the backbone tree (reference *SI Appendix*, Table S5 for details).

Diversification Rate Analyses. We applied the SFBD model (73, 74) to infer the diversification and fossil-sampling rate changes over time, using Supertrees 1 through 3 as input. This method allows for a joint estimation of net diversification rate (speciation rate minus extinction rate), relative extinction rate (extinction rate over speciation rate), and relative fossil-sampling rate (fossil sampling rate divided by the sum of extinction and fossil-sampling rates) across different time intervals. Extant taxa were assumed to be sampled uniformly at random, and the sampling proportion was set to 0.023 for Supertree 1 and 0.02 for Supertrees 2 and 3, based on the number of described extant species of birds at around 10,000. To examine the robustness of the rate estimates to the prior changes, we used different parameters in the exponential priors for the net diversification rate [exponential (50), exponential (20), and exponential (10)] and beta priors for the relative extinction and fossil-sampling rates (beta [1, 1], beta [2, 2], beta [1, 4], and beta [4, 1]). Time was binned into 33 equal-duration intervals of 5 My each. The results are given in *SI Appendix*, Figs. S6–S8 and Tables S6 and S7. We also applied the MTBD model (39, 41) implemented in Beast2 (40) to estimate the diversification rate based on Supertrees 1 through 3, and the details for parameter settings and results are given in *SI Appendix*, Figs. S12–S20.

Morphological Evolution Rate Analyses. Our evolutionary rate analyses were performed on a discrete character matrix modified from the matrix in ref. 7 from which we estimated the tree topology, divergence times, and evolutionary rates simultaneously using the Bayesian tip-dating approach. The character matrix was partitioned into six anatomical modules—skull, axial skeleton (including vertebrae, ribs, and gastralia), pectoral girdle (including pectoral girdle, sternum, and furcula), forelimb, pelvis, and hindlimb. Each partition was allowed to have independent rate variation across branches, following either the white noise (WN) (75) or independent lognormal (76) relaxed clock model, in order to assess evolutionary rate heterogeneity across modules. We used the Markov k-states variable (Mkv) model (77) with gamma-rate variation across all characters (78) for the likelihood calculation. The timetree was assigned a uniform prior (79), and the root age had an offset exponential prior with a mean of 181 Ma and a minimum of 177 Ma. The fossil ages obtained from PBDB were assigned uniform priors. Both *Allosaurus fragilis* and *Sinraptor dongi* were treated as outgroups. In consideration of the phylogenetic uncertainty within Paraves, we repeated our analyses with a monophyletic Avialae + Dromaeosauridae or Avialae + Deinonychosauria phylogenetic constraint. We also conducted analyses based on the unpartitioned matrix to test whether the pattern of morphological evolution was similar to those recovered in previous studies (8).

Morphospace Analyses. We performed the morphospace analyses on the same dataset with the six character partitions used in the evolutionary rate analyses. Both the Maximum Observable Rescaled Distance (MORD) matrix and Generalized Euclidean Distance (GED) matrix were calculated based on each partition's cladistic matrix (80, 81). We then applied the principal coordinate analysis with either MORD or GED matrix to ordinate all coelurosaurians into a multivariate morphospace. Two disparity metrics were used to evaluate the volume of the morphospace, including the sum and product of the variances. For each of the clades, we used a permutation test (two tailed) to test the null hypothesis of no difference between birds and the clade being compared (*SI Appendix*, Tables S1 and S2). We also performed a suit of sample size–corrected permutation tests with two more disparity metrics included (sum of ranges and product of ranges), and the results are given in *SI Appendix*, Figs. S26–S39. PERMANOVA (one tailed) was used to test the overlap in morphospace occupation between birds and other coelurosaurian clades (*SI Appendix*, Table S3). We also repeated our analyses on the unpartitioned cladistic matrix. Finally, we performed a suit of comparative distance tests to compare the relative differences between the difference of Mesozoic birds and their closely-related clades and that of other coelurosarian groups and their closely-related clades (*SI Appendix*, Table S4).

Code Availability. The tip-dating and diversification-rate analyses were performed using MrBayes 3.2.8 (82). Polytomy resolution and supertree assembly was accomplished in Mesquite 3.6 (83). The statistical tests in the morphospace analyses were performed in R 3.6.1 (84). Scripts for disparity analyses, Beast2 commands for lineage-specific multitype birth–death model analyses and MrBayes commands for tip-dating, diversification-rate, and morphological evolution-rate analyses are available at https://doi.org/10.6084/m9.figshare.12666338.

Data Availability. The datasets including character matrix for tip dating and nexus files for supertrees used in this study are available on Figshare (https://doi.org/10.6084/m9.figshare.12666338). All other study data are included in the article and/or *SI Appendix*.

ACKNOWLEDGMENTS. We thank Thomas Stidham for editing and commenting on the manuscript; Yuan Zhang and Yi Guo for helpful suggestions on permutation tests; Tanja Stadler for discussions on identifiability issues in the FBD model; Joëlle Barido-Sottani for using the MTBD model in Beast2; Wei Wang, Min Wang, and Shiying Wang for discussions on Mesozoic birds; Jinzhuang Xue on fossil plants; and Minghui Ren for refining the figures. This study was supported by the Hundred Young Talents Program of Chinese Academy of Sciences and the Strategic Priority Research Program of Chinese Academy of Sciences (XDB26000000) to C.Z. and the National Natural Science Foundation of China (Grant Number 41688103) and the Strategic Priority Research Program of the Chinese Academy of Sciences (XDB18000000) to X.X.

1. D. Moen, H. Morlon, From dinosaurs to modern bird diversity: Extending the time scale of adaptive radiation. *PLoS Biol.* **12**, e1001854 (2014).
2. E. Dunne, Patterns in Palaeontology: How do we measure biodiversity in the past? *Palaeontology Online* **8**, 1–9 (2018).
3. S. Claramunt, J. Cracraft, A new time tree reveals Earth history's imprint on the evolution of modern birds. *Sci. Adv.* **1**, e1501005 (2015).
4. W. Jetz, G. H. Thomas, J. B. Joy, K. Hartmann, A. O. Mooers, The global diversity of birds in space and time. *Nature* **491**, 444–448 (2012).
5. R. O. Prum *et al*., A comprehensive phylogeny of birds (Aves) using targeted next-generation DNA sequencing. *Nature* **526**, 569–573 (2015).
6. R. B. Benson, J. N. Choiniere, Rates of dinosaur limb evolution provide evidence for exceptional radiation in Mesozoic birds. *Proc. Biol. Sci.* **280**, 20131780 (2013).
7. S. L. Brusatte, G. T. Lloyd, S. C. Wang, M. A. Norell, Gradual assembly of avian body plan culminated in rapid rates of evolution across the dinosaur-bird transition. *Curr. Biol.* **24**, 2386–2392 (2014).
8. M. S. Y. Lee, A. Cau, D. Naish, G. J. Dyke, Dinosaur evolution. Sustained miniaturization and anatomical innovation in the dinosaurian ancestors of birds. *Science* **345**, 562–566 (2014).
9. M. Wang, G. T. Lloyd, Rates of morphological evolution are heterogeneous in Early Cretaceous birds. *Proc. Biol. Sci.* **283**, 20160214 (2016).
10. C. Zhang, M. Wang, Bayesian tip dating reveals heterogeneous morphological clocks in Mesozoic birds. *R. Soc. Open Sci.* **6**, 182062 (2019).
11. D. J. Field, J. Benito, A. Chen, J. W. M. Jagt, D. T. Ksepka, Late Cretaceous neornithine from Europe illuminates the origins of crown birds. *Nature* **579**, 397–401 (2020).
12. D. T. Ksepka, T. A. Stidham, T. E. Williamson, Early Paleocene landbird supports rapid phylogenetic and morphological diversification of crown birds after the K-Pg mass extinction. *Proc. Natl. Acad. Sci. U.S.A.* **114**, 8047–8052 (2017).
13. N. R. Longrich, T. Tokaryk, D. J. Field, Mass extinction of birds at the cretaceous-paleogene (K-Pg) boundary. *Proc. Natl. Acad. Sci. U.S.A.* **108**, 15253–15257 (2011).
14. T. H. Worthy, F. J. Degrange, W. D. Handley, M. S. Y. Lee, The evolution of giant flightless birds and novel phylogenetic relationships for extinct fowl (Aves, Galloanseres). *R. Soc. Open Sci.* **4**, 170975 (2017).
15. R. J. Butler, P. M. Barrett, S. Nowbath, P. Upchurch, Estimating the effects of sampling biases on pterosaur diversity patterns: Implications for hypotheses of bird/pterosaur competitive replacement. *Paleobiology* **35**, 432–446 (2009).
16. M. Sakamoto, M. J. Benton, C. Venditti, Dinosaurs in decline tens of millions of years before their final extinction. *Proc. Natl. Acad. Sci. U.S.A.* **113**, 5036–5040 (2016).
17. K. E. Omland, Correlated rates of molecular and morphological evolution. *Evolution* **51**, 1381–1393 (1997).
18. L. Bromham, M. Woolfit, M. S. Lee, A. Rambaut, Testing the relationship between morphological and molecular rates of change along phylogenies. *Evolution* **56**, 1921–1930 (2002).
19. T. J. Davies, V. Savolainen, Neutral theory, phylogenies, and the relationship between phenotypic change and evolutionary rates. *Evolution* **60**, 476–483 (2006).
20. H. Seligmann, Positive correlations between molecular and morphological rates of evolution. *J. Theor. Biol.* **264**, 799–807 (2010).
21. M. Barrier, R. H. Robichaux, M. D. Purugganan, Accelerated regulatory gene evolution in an adaptive radiation. *Proc. Natl. Acad. Sci. U.S.A.* **98**, 10208–10213 (2001).
22. F. T. Burbrink, X. Chen, E. A. Myers, M. C. Brandley, R. A. Pyron, Evidence for determinism in species diversification and contingency in phenotypic evolution during adaptive radiation. *Proc. Biol. Sci.* **279**, 4817–4826 (2012).
23. D. C. Adams, C. M. Berns, K. H. Kozak, J. J. Wiens, Are rates of species diversification correlated with rates of morphological evolution? *Proc. Biol. Sci.* **276**, 2729–2738 (2009).

24. D. L. Rabosky *et al*., Rates of speciation and morphological evolution are correlated across the largest vertebrate radiation. *Nat. Commun.* **4**, 1958 (2013).
25. N. M. A. Crouch, R. E. Ricklefs, Speciation rate is independent of the rate of evolution of morphological size, shape, and absolute morphological specialization in a large clade of birds. *Am. Nat.* **193**, E78–E91 (2019).
26. M. Conway, B. J. Olsen, Contrasting drivers of diversification rates on islands and continents across three passerine families. *Proc. Biol. Sci.* **286**, 20191757 (2019).
27. D. L. Rabosky, D. C. Adams, Rates of morphological evolution are correlated with species richness in salamanders. *Evolution* **66**, 1807–1818 (2012).
28. S. H. Eo, J. A. DeWoody, Evolutionary rates of mitochondrial genomes correspond to diversification rates and to contemporary species richness in birds and reptiles. *Proc. Biol. Sci.* **277**, 3587–3592 (2010).
29. M. Iglesias-Carrasco, M. D. Jennions, S. Y. W. Ho, D. A. Duchêne, Sexual selection, body mass and molecular evolution interact to predict diversification in birds. *Proc. Biol. Sci.* **286**, 20190172 (2019).
30. J. Janecka, B. Chowdhary, W. Murphy, Exploring the correlations between sequence evolution rate and phenotypic divergence across the Mammalian tree provides insights into adaptive evolution. *J. Biosci.* **37**, 897–909 (2012).
31. C. J. Law, G. J. Slater, R. S. Mehta, Lineage diversity and size disparity in Musteloidea: Testing patterns of adaptive radiation using molecular and fossil-based methods. *Syst. Biol.* **67**, 127–144 (2018).
32. X. Goldie, R. Lanfear, L. Bromham, Diversification and the rate of molecular evolution: No evidence of a link in mammals. *BMC Evol. Biol.* **11**, 286 (2011).
33. D. J. Field *et al*., Early evolution of modern birds structured by global forest collapse at the end-Cretaceous mass extinction. *Curr. Biol.* **28**, 1825–1831.e2 (2018).
34. A. Feduccia, Explosive evolution in tertiary birds and mammals. *Science* **267**, 637–638 (1995).
35. A. Feduccia, 'Big bang' for tertiary birds? *Trends Ecol. Evol.* **18**, 172–176 (2003).
36. A. Feduccia, Avian extinction at the end of the Cretaceous: Assessing the magnitude and subsequent explosive radiation. *Cretac. Res.* **50**, 1–15 (2014).
37. R. T. Kimball, C. H. Oliveros, N. Wang, N. D. White, E. L. Braun, A phylogenomic supertree of birds. *Diversity (Basel)* **11**, 109 (2019).
38. E. D. Jarvis *et al*., Whole-genome analyses resolve early branches in the tree of life of modern birds. *Science* **346**, 1320–1331 (2014).
39. J. Barido-Sottani, T. G. Vaughan, T. Stadler, A multitype birth–death model for bayesian inference of lineage-specific birth and death rates. *Syst. Biol.* **69**, 973–986 (2020).
40. R. Bouckaert *et al*., BEAST 2.5: An advanced software platform for Bayesian evolutionary analysis. *PLoS Comput. Biol.* **15**, e1006650 (2019).
41. J. S. Mitchell, R. S. Etienne, D. L. Rabosky, Inferring diversification rate variation from phylogenies with fossils. *Syst. Biol.* **68**, 1–18 (2019).
42. N. Brocklehurst, P. Upchurch, P. D. Mannion, J. O'Connor, The completeness of the fossil record of mesozoic birds: Implications for early avian evolution. *PLoS One* **7**, e39056 (2012).
43. X. Xu *et al*., An integrative approach to understanding bird origins. *Science* **346**, 1253293 (2014).
44. L. E. Zanno, P. J. Makovicky, Herbivorous ecomorphology and specialization patterns in theropod dinosaur evolution. *Proc. Natl. Acad. Sci. U.S.A.* **108**, 232–237 (2011).
45. Q. Li *et al*., Melanosome evolution indicates a key physiological shift within feathered dinosaurs. *Nature* **507**, 350–353 (2014).
46. A. Cau, The assembly of the avian body plan: A 160-million-year long process. *Boll. Soc. Paleontol. Ital.* **57**, 1–25 (2018).
47. M. N. Puttick, G. H. Thomas, M. J. Benton, High rates of evolution preceded the origin of birds. *Evolution* **68**, 1497–1510 (2014).
48. T. A. Dececchi, H. C. E. Larsson, Patristic evolutionary rates suggest a punctuated pattern in forelimb evolution before and after the origin of birds. *Paleobiology* **35**, 1–12 (2009).
49. A. Prieto-Marquez, T. L. Stubbs, M. J. Benton, S. Brusatte, Regional morphological disparity and rates of evolution in coelurosaurian theropod dinosaurs. *J. Vertebr. Paleontol.* **36**, 208A (2016).
50. A. Bell, L. M. Chiappe, Statistical approach for inferring ecology of Mesozoic birds. *J. Syst. Palaeontology* **9**, 119–133 (2011).
51. R. A. Close, E. J. Rayfield, Functional morphometric analysis of the furcula in mesozoic birds. *PLoS One* **7**, e36664 (2012).
52. G. J. Dyke, R. L. Nudds, The fossil record and limb disparity of enantiornithines, the dominant flying birds of the Cretaceous. *Lethaia* **42**, 248–254 (2009).
53. F. J. Serrano, P. Palmqvist, L. M. Chiappe, J. L. Sanz, Inferring flight parameters of Mesozoic avians through multivariate analyses of forelimb elements in their living relatives. *Paleobiology* **43**, 144–169 (2016).
54. J. P. Tennant, P. D. Mannion, P. Upchurch, M. D. Sutton, G. D. Price, Biotic and environmental dynamics through the late Jurassic-early cretaceous transition: Evidence for protracted faunal and ecological turnover. *Biol. Rev. Camb. Philos. Soc.* **92**, 776–814 (2017).
55. H. Hu *et al*., Evolution of the vomer and its implications for cranial kinesis in Paraves. *Proc. Natl. Acad. Sci. U.S.A.* **116**, 19571–19578 (2019).
56. J. W. Brown, R. B. Payne, D. P. Mindell, Nuclear DNA does not reconcile 'rocks' and 'clocks' in Neoaves: A comment on Ericson et al. *Biol. Lett.* **3**, 257–260 (2007).
57. M. Van Tuinen, T. A. Stidham, E. A. Hadly, Tempo and mode of modern bird evolution observed with large-scale taxonomic Sampling. *Hist. Biol.* **18**, 205–221 (2006).
58. G. Mayr, The Paleogene fossil record of birds in Europe. *Biol. Rev. Camb. Philos. Soc.* **80**, 515–542 (2005).
59. M. J. Benton, The origins of modern biodiversity on land. *Philos. Trans. R. Soc. Lond. B Biol. Sci.* **365**, 3667–3679 (2010).
60. H. Song, P. B. Wignall, H. Song, X. Dai, D. Chu, Seawater temperature and dissolved oxygen over the past 500 million years. *J. Earth Sci.* **30**, 236–243 (2019).
61. J. T. Parrish, F. Peterson, C. E. Turner, Jurassic "savannah"—plant taphonomy and climate of the Morrison formation (upper Jurassic, Western USA). *Sediment. Geol.* **167**, 137–162 (2004).
62. P. M. Rees, C. Noto, J. M. Parrish, J. Parrish, Late Jurassic climates, vegetation, and dinosaur distributions. *J. Geol.* **112**, 643–653 (2004).
63. C. C. Davis, C. O. Webb, K. J. Wurdack, C. A. Jaramillo, M. J. Donoghue, Explosive radiation of Malpighiales supports a mid-cretaceous origin of modern tropical rain forests. *Am. Nat.* **165**, E36–E65 (2005).
64. K. Feldberg *et al*., Epiphytic leafy liverworts diversified in angiosperm-dominated forests. *Sci. Rep.* **4**, 5974 (2014).
65. N. A. Jud *et al*., A new fossil assemblage shows that large angiosperm trees grew in North America by the Turonian (Late Cretaceous). *Sci. Adv.* **4**, eaar8568 (2018).
66. H. Schneider *et al*., Ferns diversified in the shadow of angiosperms. *Nature* **428**, 553–557 (2004).
67. G. P. Wilson *et al*., Adaptive radiation of multituberculate mammals before the extinction of dinosaurs. *Nature* **483**, 457–460 (2012).
68. M. Chen, C. A. E. Strömberg, G. P. Wilson, Assembly of modern mammal community structure driven by Late Cretaceous dental evolution, rise of flowering plants, and dinosaur demise. *Proc. Natl. Acad. Sci. U.S.A.* **116**, 9931–9940 (2019).
69. O. Friedrich, R. D. Norris, J. Erbacher, Evolution of middle to Late Cretaceous oceans—A 55 m.y. record of Earth's temperature and carbon cycle. *Geology* **40**, 107–110 (2012).
70. N. R. Longrich, D. M. Martill, B. Andres, Late Maastrichtian pterosaurs from North Africa and mass extinction of Pterosauria at the Cretaceous-Paleogene boundary. *PLoS Biol.* **16**, e2001663 (2018).
71. S. Louca, M. W. Pennell, Extant timetrees are consistent with a myriad of diversification histories. *Nature* **580**, 502–505 (2020).
72. T. Stadler, D. Kühnert, S. Bonhoeffer, A. J. Drummond, Birth-death skyline plot reveals temporal changes of epidemic spread in HIV and hepatitis C virus (HCV). *Proc. Natl. Acad. Sci. U.S.A.* **110**, 228–233 (2013).
73. A. Gavryushkina, D. Welch, T. Stadler, A. J. Drummond, Bayesian inference of sampled ancestor trees for epidemiology and fossil calibration. *PLoS Comput. Biol.* **10**, e1003919 (2014).
74. C. Zhang, T. Stadler, S. Klopfstein, T. A. Heath, F. Ronquist, Total-evidence dating under the fossilized birth-death process. *Syst. Biol.* **65**, 228–249 (2016).
75. T. Lepage, D. Bryant, H. Philippe, N. Lartillot, A general comparison of relaxed molecular clock models. *Mol. Biol. Evol.* **24**, 2669–2680 (2007).
76. A. J. Drummond, S. Y. Ho, M. J. Phillips, A. Rambaut, Relaxed phylogenetics and dating with confidence. *PLoS Biol.* **4**, e88 (2006).
77. P. O. Lewis, A likelihood approach to estimating phylogeny from discrete morphological character data. *Syst. Biol.* **50**, 913–925 (2001).
78. Z. Yang, Maximum likelihood phylogenetic estimation from DNA sequences with variable rates over sites: Approximate methods. *J. Mol. Evol.* **39**, 306–314 (1994).
79. F. Ronquist *et al*., A total-evidence approach to dating with fossils, applied to the early radiation of the hymenoptera. *Syst. Biol.* **61**, 973–999 (2012).
80. G. T. Lloyd, Estimating morphological diversity and tempo with discrete character-taxon matrices: Implementation, challenges, progress, and future directions. *Biol. J. Linn. Soc. Lond.* **118**, 131–151 (2016).
81. M. A. Wills, Crustacean disparity through the Phanerozoic: Comparing morphological and stratigraphic data. *Biol. J. Linn. Soc. Lond.* **65**, 455–500 (1998).
82. F. Ronquist *et al*., MrBayes 3.2: Efficient Bayesian phylogenetic inference and model choice across a large model space. *Syst. Biol.* **61**, 539–542 (2012).
83. M. Wayne, M. David, Mesquite: A Modular System for Evolutionary Analysis (Version 3.61, 2019). http://www.mesquiteproject.org. Accessed 9 February 2021.
84. RCoreTeam, *R: A Language and Environment for Statistical Computing* (R Foundation for Statistical Computing, Vienna, Austria, 2019).